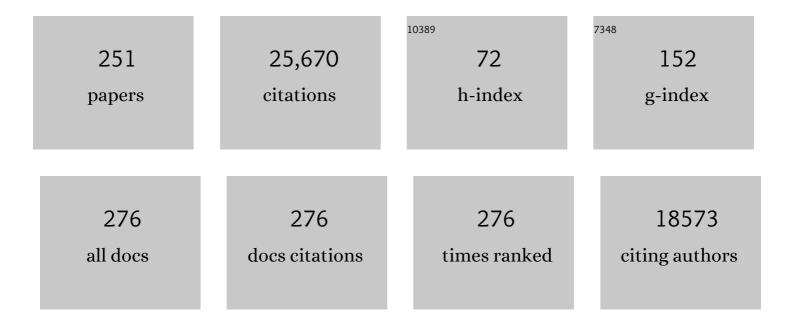
Ravi S Menon

List of Publications by Year in descending order

Source: https://exaly.com/author-pdf/6183662/publications.pdf Version: 2024-02-01



#	Article	IF	CITATIONS
1	Intrinsic signal changes accompanying sensory stimulation: functional brain mapping with magnetic resonance imaging Proceedings of the National Academy of Sciences of the United States of America, 1992, 89, 5951-5955.	7.1	3,216
2	Functional brain mapping by blood oxygenation level-dependent contrast magnetic resonance imaging. A comparison of signal characteristics with a biophysical model. Biophysical Journal, 1993, 64, 803-812.	0.5	1,620
3	Dissociating Pain from Its Anticipation in the Human Brain. Science, 1999, 284, 1979-1981.	12.6	1,026
4	Resting-state networks show dynamic functional connectivity in awake humans and anesthetized macaques. Human Brain Mapping, 2013, 34, 2154-2177.	3.6	667
5	Visually guided grasping produces fMRI activation in dorsal but not ventral stream brain areas. Experimental Brain Research, 2003, 153, 180-189.	1.5	636
6	Imaging Attentional Modulation of Pain in the Periaqueductal Gray in Humans. Journal of Neuroscience, 2002, 22, 2748-2752.	3.6	527
7	Experimental determination of the BOLD field strength dependence in vessels and tissue. Magnetic Resonance in Medicine, 1997, 38, 296-302.	3.0	474
8	Neural Correlates of Traumatic Memories in Posttraumatic Stress Disorder: A Functional MRI Investigation. American Journal of Psychiatry, 2001, 158, 1920-1922.	7.2	473
9	Brain activation during script-driven imagery induced dissociative responses in PTSD: a functional magnetic resonance imaging investigation. Biological Psychiatry, 2002, 52, 305-311.	1.3	470
10	Motor Area Activity During Mental Rotation Studied by Time-Resolved Single-Trial fMRI. Journal of Cognitive Neuroscience, 2000, 12, 310-320.	2.3	461
11	BOLD Based Functional MRI at 4 Tesla Includes a Capillary Bed Contribution: Echo-Planar Imaging Correlates with Previous Optical Imaging Using Intrinsic Signals. Magnetic Resonance in Medicine, 1995, 33, 453-459.	3.0	407
12	4 Tesla gradient recalled echo characteristics of photic stimulation-induced signal changes in the human primary visual cortex. Magnetic Resonance in Medicine, 1993, 30, 380-386.	3.0	405
13	Glutamate and Glutamine Measured With 4.0 T Proton MRS in Never-Treated Patients With Schizophrenia and Healthy Volunteers. American Journal of Psychiatry, 2002, 159, 1944-1946.	7.2	386
14	Haptic study of three-dimensional objects activates extrastriate visual areas. Neuropsychologia, 2002, 40, 1706-1714.	1.6	367
15	Cerebral Cortical Representation of Automatic and Volitional Swallowing in Humans. Journal of Neurophysiology, 2001, 85, 938-950.	1.8	345
16	Functional imaging of human motor cortex at high magnetic field. Journal of Neurophysiology, 1993, 69, 297-302.	1.8	339
17	Human fMRI evidence for the neural correlates of preparatory set. Nature Neuroscience, 2002, 5, 1345-1352.	14.8	319
18	Recall of emotional states in posttraumatic stress disorder: an fMRI investigation. Biological Psychiatry, 2003, 53, 204-210.	1.3	299

#	Article	IF	CITATIONS
19	ON THE CHARACTERISTICS OF FUNCTIONAL MAGNETIC RESONANCE IMAGING OF THE BRAIN. Annual Review of Biophysics and Biomolecular Structure, 1998, 27, 447-474.	18.3	285
20	A Comparison of Frontoparietal fMRI Activation During Anti-Saccades and Anti-Pointing. Journal of Neurophysiology, 2000, 84, 1645-1655.	1.8	283
21	Ocular Dominance in Human V1 Demonstrated by Functional Magnetic Resonance Imaging. Journal of Neurophysiology, 1997, 77, 2780-2787.	1.8	282
22	Differential Effects of Viewpoint on Object-Driven Activation in Dorsal and Ventral Streams. Neuron, 2002, 35, 793-801.	8.1	258
23	Glutamate and Glutamine in the Anterior Cingulate and Thalamus of Medicated Patients With Chronic Schizophrenia and Healthy Comparison Subjects Measured With 4.0-T Proton MRS. American Journal of Psychiatry, 2003, 160, 2231-2233.	7.2	254
24	Cerebral Areas Processing Swallowing and Tongue Movement Are Overlapping but Distinct: A Functional Magnetic Resonance Imaging Study. Journal of Neurophysiology, 2004, 92, 2428-2443.	1.8	252
25	Distinguishing Subregions of the Human MT+ Complex Using Visual Fields and Pursuit Eye Movements. Journal of Neurophysiology, 2001, 86, 1991-2000.	1.8	251
26	Noise Reduction in BOLD-Based fMRI Using Component Analysis. NeuroImage, 2002, 17, 1521-1537.	4.2	248
27	Functional connectivity of dissociative responses in posttraumatic stress disorder: A functional magnetic resonance imaging investigation. Biological Psychiatry, 2005, 57, 873-884.	1.3	238
28	An fMRI study of the selective activation of human extrastriate form vision areas by radial and concentric gratings. Current Biology, 2000, 10, 1455-1458.	3.9	237
29	Preparatory Set Associated With Pro-Saccades and Anti-Saccades in Humans Investigated With Event-Related fMRI. Journal of Neurophysiology, 2003, 89, 1016-1023.	1.8	234
30	Mental chronometry using latency-resolved functional MRI. Proceedings of the National Academy of Sciences of the United States of America, 1998, 95, 10902-10907.	7.1	228
31	High contrast and fast threeâ€dimensional magnetic resonance imaging at high fields. Magnetic Resonance in Medicine, 1995, 34, 308-312.	3.0	225
32	The Nature of Traumatic Memories: A 4-T fMRI Functional Connectivity Analysis. American Journal of Psychiatry, 2004, 161, 36-44.	7.2	224
33	Postacquisition suppression of large-vessel BOLD signals in high-resolution fMRI. Magnetic Resonance in Medicine, 2002, 47, 1-9.	3.0	194
34	Ventral medial prefrontal cortex and cardiovagal control in conscious humans. NeuroImage, 2007, 35, 698-708.	4.2	194
35	An Open Resource for Non-human Primate Imaging. Neuron, 2018, 100, 61-74.e2.	8.1	190
36	Cortical regions associated with autonomic cardiovascular regulation during lower body negative pressure in humans. Journal of Physiology, 2005, 569, 331-345.	2.9	185

#	Article	IF	CITATIONS
37	Spatial and temporal limits in cognitive neuroimaging with fMRI. Trends in Cognitive Sciences, 1999, 3, 207-216.	7.8	182
38	Human forebrain activation by visceral stimuli. , 1999, 413, 572-582.		179
39	Longitudinal grey-matter and glutamatergic losses in first-episode schizophrenia. British Journal of Psychiatry, 2007, 191, 325-334.	2.8	176
40	The effects of visual object priming on brain activation before and after recognition. Current Biology, 2000, 10, 1017-1024.	3.9	161
41	Submillimeter functional localization in human striate cortex using BOLD contrast at 4 Tesla: Implications for the vascular point-spread function. Magnetic Resonance in Medicine, 1999, 41, 230-235.	3.0	155
42	Novelty responses to relational and non-relational information in the hippocampus and the parahippocampal region: A comparison based on event-related fMRI. Hippocampus, 2005, 15, 763-774.	1.9	149
43	A transmit-only/receive-only (TORO) RF system for high-field MRI/MRS applications. Magnetic Resonance in Medicine, 2000, 43, 284-289.	3.0	141
44	Brief visual stimulation allows mapping of ocular dominance in visual cortex using fMRI. Human Brain Mapping, 2001, 14, 210-217.	3.6	139
45	Identification of Optimal Structural Connectivity Using Functional Connectivity and Neural Modeling. Journal of Neuroscience, 2014, 34, 7910-7916.	3.6	138
46	Flexible Retinotopy: Motion-Dependent Position Coding in the Visual Cortex. Science, 2003, 302, 878-881.	12.6	136
47	An NMR determination of the physiological water distribution in wood during drying. Journal of Applied Polymer Science, 1987, 33, 1141-1155.	2.6	132
48	Resting-state networks in the macaque at 7T. NeuroImage, 2011, 56, 1546-1555.	4.2	131
49	Application of continuous relaxation time distributions to the fitting of data from model systmes and excised tissue. Magnetic Resonance in Medicine, 1991, 20, 214-227.	3.0	130
50	Comparison of the quantification precision of human short echo time1H spectroscopy at 1.5 and 4.0 Tesla. Magnetic Resonance in Medicine, 2000, 44, 185-192.	3.0	128
51	A 4.0-T fMRI study of brain connectivity during word fluency in first-episode schizophrenia. Schizophrenia Research, 2005, 75, 247-263.	2.0	124
52	Isoflurane induces dose-dependent alterations in the cortical connectivity profiles and dynamic properties of the brain's functional architecture. Human Brain Mapping, 2014, 35, 5754-5775.	3.6	122
53	Eye Position Signal Modulates a Human Parietal Pointing Region during Memory-Guided Movements. Journal of Neuroscience, 2000, 20, 5835-5840.	3.6	120
54	Predictors of highly prevalent brain ischemia in intracerebral hemorrhage. Annals of Neurology, 2012, 71, 199-205.	5.3	119

#	Article	IF	CITATIONS
55	Differences in perceived shape from shading correlate with activity in early visual areas. Current Biology, 1997, 7, 144-147.	3.9	115
56	Functional connectivity of the frontal eye fields in humans and macaque monkeys investigated with resting-state fMRI. Journal of Neurophysiology, 2012, 107, 2463-2474.	1.8	112
57	Cerebral cortical processing of swallowing in older adults. Experimental Brain Research, 2006, 176, 12-22.	1.5	109
58	A sensitive PARACEST contrast agent for temperature MRI: Eu ³⁺ â€DOTAMâ€glycine (Gly)â€phenylalanine (Phe). Magnetic Resonance in Medicine, 2008, 59, 374-381.	3.0	106
59	Information Processing Architecture of Functionally Defined Clusters in the Macaque Cortex. Journal of Neuroscience, 2012, 32, 17465-17476.	3.6	106
60	Theoretical and Experimental Optimization of Laser Speckle Contrast Imaging for High Specificity to Brain Microcirculation. Journal of Cerebral Blood Flow and Metabolism, 2007, 27, 258-269.	4.3	105
61	Grey matter and social functioning correlates of glutamatergic metabolite loss in schizophrenia. British Journal of Psychiatry, 2011, 198, 448-456.	2.8	103
62	Recovery of fMRI Activation in Motion Area MT Following Storage of the Motion Aftereffect. Journal of Neurophysiology, 1999, 81, 388-393.	1.8	102
63	Comparison of Memory- and Visually Guided Saccades Using Event-Related fMRI. Journal of Neurophysiology, 2004, 91, 873-889.	1.8	99
64	BOLD fMRI Response of Early Visual Areas to Perceived Contrast in Human Amblyopia. Journal of Neurophysiology, 2000, 84, 1907-1913.	1.8	98
65	Functional Brain Mapping Using Magnetic Resonance Imaging: Signal Changes Accompanying Visual Stimulation. Investigative Radiology, 1992, 27, S47-S53.	6.2	97
66	31P magnetic resonance spectroscopy of the Sherpa heart: a phosphocreatine/adenosine triphosphate signature of metabolic defense against hypobaric hypoxia Proceedings of the National Academy of Sciences of the United States of America, 1996, 93, 1215-1220.	7.1	96
67	Learning-related fMRI activation associated with a rotational visuo-motor transformation. Cognitive Brain Research, 2005, 22, 373-383.	3.0	93
68	Accelerating the Evolution of Nonhuman Primate Neuroimaging. Neuron, 2020, 105, 600-603.	8.1	92
69	Proton Relaxation Studies of Water Compartmentalization in a Model Neurological System. Magnetic Resonance in Medicine, 1992, 28, 264-274.	3.0	87
70	Discrete functional contributions of cerebral cortical foci in voluntary swallowing: a functional magnetic resonance imaging (fMRI) ?Go, No-Go? study. Experimental Brain Research, 2005, 161, 81-90.	1.5	84
71	Robust automated shimming technique using arbitrary mapping acquisition parameters (RASTAMAP). Magnetic Resonance in Medicine, 2004, 51, 881-887.	3.0	83
72	Multiparametric MRI changes persist beyond recovery in concussed adolescent hockey players. Neurology, 2017, 89, 2157-2166.	1.1	83

Ravi S Menon

#	Article	IF	CITATIONS
73	Behavioral and Neuroimaging Evidence for a Contribution of Color and Texture Information to Scene Classification in a Patient with Visual Form Agnosia. Journal of Cognitive Neuroscience, 2004, 16, 955-965.	2.3	80
74	Elimination of the Vesicular Acetylcholine Transporter in the Striatum Reveals Regulation of Behaviour by Cholinergic-Glutamatergic Co-Transmission. PLoS Biology, 2011, 9, e1001194.	5.6	80
75	Functional MRI of oropharyngeal air-pulse stimulation. Neuroscience, 2008, 153, 1300-1308.	2.3	79
76	Effect of Luminance Contrast on BOLD fMRI Response in Human Primary Visual Areas. Journal of Neurophysiology, 1998, 79, 2204-2207.	1.8	78
77	Frontoparietal Functional Connectivity in the Common Marmoset. Cerebral Cortex, 2017, 27, 3890-3905.	2.9	78
78	Spectroscopic lineshape correction by QUECC: Combined QUALITY deconvolution and eddy current correction. Magnetic Resonance in Medicine, 2000, 44, 641-645.	3.0	76
79	Divergence of rodent and primate medial frontal cortex functional connectivity. Proceedings of the National Academy of Sciences of the United States of America, 2020, 117, 21681-21689.	7.1	76
80	An MRI study of subgenual prefrontal cortex in patients with familial and non-familial bipolar I disorder. Journal of Affective Disorders, 2003, 77, 167-171.	4.1	73
81	Individual Differences in a Husband and Wife Who Developed PTSD After a Motor Vehicle Accident: A Functional MRI Case Study. American Journal of Psychiatry, 2003, 160, 667-669.	7.2	73
82	Amplitude response and stimulus presentation frequency response of human primary visual cortex using BOLD EPI at 4 T. Magnetic Resonance in Medicine, 1998, 40, 203-209.	3.0	72
83	Simultaneous in vivo pH and temperature mapping using a PARACESTâ€MRI contrast agent. Magnetic Resonance in Medicine, 2013, 70, 1016-1025.	3.0	66
84	In vivo brain31P-MRS: measuring the phospholipid resonances at 4 Tesla from small voxels. NMR in Biomedicine, 2002, 15, 338-347.	2.8	64
85	Human cardiovascular and gustatory brainstem sites observed by functional magnetic resonance imaging. Journal of Comparative Neurology, 2004, 471, 446-461.	1.6	62
86	Sex differences in forebrain and cardiovagal responses at the onset of isometric handgrip exercise: a retrospective fMRI study. Journal of Applied Physiology, 2007, 103, 1402-1411.	2.5	62
87	31P NMR spectroscopy of the human heart at 4 T: Detection of substantially uncontaminated cardiac spectra and differentiation of subepicardium and subendocardium. Magnetic Resonance in Medicine, 1992, 26, 368-376.	3.0	61
88	Resting-State Connectivity Identifies Distinct Functional Networks in Macaque Cingulate Cortex. Cerebral Cortex, 2012, 22, 1294-1308.	2.9	61
89	Transient hemodynamics during a breath hold challenge in a two part functional imaging study with simultaneous near-infrared spectroscopy in adult humans. NeuroImage, 2003, 20, 1246-1252.	4.2	59
90	Sliceâ€byâ€slice <i>B</i> ₁ ⁺ shimming at 7 T. Magnetic Resonance in Medicine, 2012, 68, 1109-1116.	3.0	58

#	Article	IF	CITATIONS
91	Origins of <i>R</i> ₂ ^{â^—} orientation dependence in gray and white matter. Proceedings of the National Academy of Sciences of the United States of America, 2014, 111, E159-67.	7.1	54
92	Imaging outcome measures of neuroprotection and repair in MS. Neurology, 2019, 92, 519-533.	1.1	53
93	High resolution fMRI of ocular dominance columns within the visual cortex of human amblyopes. Strabismus, 2002, 10, 129-136.	0.7	52
94	Focal changes in brain energy and phospholipid metabolism in first-episode schizophrenia. British Journal of Psychiatry, 2004, 184, 409-415.	2.8	51
95	A conformal transceive array for 7 T neuroimaging. Magnetic Resonance in Medicine, 2012, 67, 1487-1496.	3.0	51
96	Investigation of BOLD contrast in fMRI using multi-shot EPI. NMR in Biomedicine, 1997, 10, 179-182.	2.8	50
97	Grey and white matter differences in brain energy metabolism in first episode schizophrenia: 31P-MRS chemical shift imaging at 4 Tesla. Psychiatry Research - Neuroimaging, 2006, 146, 127-135.	1.8	50
98	BOLD fMRI activation for anti-saccades in nonhuman primates. NeuroImage, 2009, 45, 470-476.	4.2	50
99	Multiple Sclerosis: Improved Identification of Disease-relevant Changes in Gray and White Matter by Using Susceptibility-based MR Imaging. Radiology, 2014, 272, 851-864.	7.3	50
100	Comparison of resting-state functional connectivity in marmosets with tracer-based cellular connectivity. NeuroImage, 2020, 204, 116241.	4.2	50
101	Region-specific changes in phospholipid metabolism in chronic, medicated schizophrenia. British Journal of Psychiatry, 2002, 180, 39-44.	2.8	49
102	Multiexponential proton relaxation in model cellular systems. Magnetic Resonance in Medicine, 1991, 20, 196-213.	3.0	46
103	Duration of untreated psychosis vs. N-acetylaspartate and choline in first episode schizophrenia: a 1H magnetic resonance spectroscopy study at 4.0 Tesla. Psychiatry Research - Neuroimaging, 2004, 131, 107-114.	1.8	46
104	Forebrain neural patterns associated with sex differences in autonomic and cardiovascular function during baroreceptor unloading. American Journal of Physiology - Regulatory Integrative and Comparative Physiology, 2007, 292, R715-R722.	1.8	46
105	fMRI evidence for an inverted face representation in human somatosensory cortex. NeuroReport, 1999, 10, 1393-1395.	1.2	45
106	Transceive surface coil array for magnetic resonance imaging of the human brain at 4 T. Magnetic Resonance in Medicine, 2005, 54, 499-503.	3.0	45
107	Integrated radiofrequency array and animal holder design for minimizing head motion during awake marmoset functional magnetic resonance imaging. NeuroImage, 2019, 193, 126-138.	4.2	45
108	Representation of Head-Centric Flow in the Human Motion Complex. Journal of Neuroscience, 2006, 26, 5616-5627.	3.6	44

#	Article	IF	CITATIONS
109	The great brain versus vein debate. NeuroImage, 2012, 62, 970-974.	4.2	43
110	Medial Prefrontal and Anterior Insular Connectivity in Early Schizophrenia and Major Depressive Disorder: A Resting Functional MRI Evaluation of Large-Scale Brain Network Models. Frontiers in Human Neuroscience, 2016, 10, 132.	2.0	43
111	Metabolomics profiling of concussion in adolescent male hockey players: a novel diagnostic method. Metabolomics, 2016, 12, 1.	3.0	43
112	A radiofrequency coil to facilitate <i>B</i> shimming and parallel imaging acceleration in three dimensions at 7 T. NMR in Biomedicine, 2011, 24, 815-823.	2.8	41
113	Repetition priming and the time course of object recognition. NeuroReport, 1999, 10, 1019-1023.	1.2	39
114	Optimized parallel transmit and receive radiofrequency coil for ultrahigh-field MRI of monkeys. NeuroImage, 2016, 125, 153-161.	4.2	39
115	Imaging function in the working brain with fMRI. Current Opinion in Neurobiology, 2001, 11, 630-636.	4.2	38
116	Perirhinal and hippocampal contributions to visual recognition memory can be distinguished from those of occipitoâ€ŧemporal structures based on conscious awareness of prior occurrence. Hippocampus, 2007, 17, 1081-1092.	1.9	38
117	Electrophysiological signatures of spontaneous BOLD fluctuations in macaque prefrontal cortex. NeuroImage, 2015, 113, 257-267.	4.2	38
118	Altered Resting-State Functional Connectivity Between Awake and Isoflurane Anesthetized Marmosets. Cerebral Cortex, 2020, 30, 5943-5959.	2.9	36
119	Task-based fMRI of a free-viewing visuo-saccadic network in the marmoset monkey. NeuroImage, 2019, 202, 116147.	4.2	35
120	Comparison of Multiple Sclerosis Cortical Lesion Types Detected by Multicontrast 3T and 7T MRI. American Journal of Neuroradiology, 2019, 40, 1162-1169.	2.4	34
121	Face selective patches in marmoset frontal cortex. Nature Communications, 2020, 11, 4856.	12.8	34
122	Long component time constant of23NaT*2 relaxation in healthy human brain. Magnetic Resonance in Medicine, 2004, 52, 407-410.	3.0	32
123	Neuroimaging Demonstration of Evolving Small Vessel Ischemic Injury in Cerebral Amyloid Angiopathy. Stroke, 2009, 40, e675-7.	2.0	32
124	Spatial and temporal resolution of functional magnetic resonance imaging. Biochemistry and Cell Biology, 1998, 76, 560-571.	2.0	31
125	Evaluation of preprocessing steps to compensate for magnetic field distortions due to body movements in BOLD fMRI. Magnetic Resonance Imaging, 2010, 28, 235-244.	1.8	31
126	Design of a Parallel Transmit Head Coil at 7T With Magnetic Wall Distributed Filters. IEEE Transactions on Medical Imaging, 2015, 34, 836-845.	8.9	31

#	Article	IF	CITATIONS
127	Repetitive mild traumatic brain injury in mice triggers a slowly developing cascade of long-term and persistent behavioral deficits and pathological changes. Acta Neuropathologica Communications, 2021, 9, 60.	5.2	31
128	Linear aspects of transformation from interictal epileptic discharges to BOLD fMRI signals in an an animal model of occipital epilepsy. NeuroImage, 2006, 30, 1133-1148.	4.2	30
129	Connectivity of the Primate Superior Colliculus Mapped by Concurrent Microstimulation and Event-Related fMRI. PLoS ONE, 2008, 3, e3928.	2.5	30
130	In vivo detection of MRIâ€PARACEST agents in mouse brain tumors at 9.4 T. Magnetic Resonance in Medicine, 2011, 66, 67-72.	3.0	30
131	Functional connectivity patterns of medial and lateral macaque frontal eye fields reveal distinct visuomotor networks. Journal of Neurophysiology, 2013, 109, 2560-2570.	1.8	30
132	Modeling and suppression of respiration-related physiological noise in echo-planar functional magnetic resonance imaging using global and one-dimensional navigator echo correction. Magnetic Resonance in Medicine, 2005, 54, 411-418.	3.0	29
133	Transmit/receive radiofrequency coil with individually shielded elements. Magnetic Resonance in Medicine, 2010, 64, 1640-1651.	3.0	29
134	EEG Monitoring during Functional MRI in Animal Models. Epilepsia, 2007, 48, 37-46.	5.1	28
135	MRI RF Array Decoupling Method With Magnetic Wall Distributed Filters. IEEE Transactions on Medical Imaging, 2015, 34, 825-835.	8.9	28
136	Exploring the limits of network topology estimation using diffusion-based tractography and tracer studies in the macaque cortex. NeuroImage, 2019, 191, 81-92.	4.2	28
137	Real-time display of artifact-free electroencephalography during functional magnetic resonance imaging and magnetic resonance spectroscopy in an animal model of epilepsy. Magnetic Resonance in Medicine, 2005, 53, 456-464.	3.0	27
138	Poor Long-Term Blood Pressure Control After Intracerebral Hemorrhage. Stroke, 2012, 43, 2580-2585.	2.0	27
139	Neuroplastic Sensorimotor Resting State Network Reorganization in Children With Hemiplegic Cerebral Palsy Treated With Constraint-Induced Movement Therapy. Journal of Child Neurology, 2016, 31, 220-226.	1.4	27
140	Resting State and Diffusion Neuroimaging Predictors of Clinical Improvements Following Constraint-Induced Movement Therapy in Children With Hemiplegic Cerebral Palsy. Journal of Child Neurology, 2015, 30, 1507-1514.	1.4	26
141	Intrinsic Functional Boundaries of Lateral Frontal Cortex in the Common Marmoset Monkey. Journal of Neuroscience, 2019, 39, 1020-1029.	3.6	26
142	Looming and receding visual networks in awake marmosets investigated with fMRI. NeuroImage, 2020, 215, 116815.	4.2	26
143	Interspecies activation correlations reveal functional correspondences between marmoset and human brain areas. Proceedings of the National Academy of Sciences of the United States of America, 2021, 118, .	7.1	26
144	Spectroscopic Imaging of Circular Voxels with a Two-Dimensional Fourier-Series Window Technique. Journal of Magnetic Resonance Series B, 1994, 105, 225-232.	1.6	25

#	Article	IF	CITATIONS
145	Forebrain regions associated with postexercise differences in autonomic and cardiovascular function during baroreceptor unloading. American Journal of Physiology - Heart and Circulatory Physiology, 2007, 293, H299-H306.	3.2	25
146	Characterization of the blood-oxygen level-dependent (BOLD) response in cat auditory cortex using high-field fMRI. NeuroImage, 2013, 64, 458-465.	4.2	25
147	There's more than one way to scan a cat: Imaging cat auditory cortex with high-field fMRI using continuous or sparse sampling. Journal of Neuroscience Methods, 2014, 224, 96-106.	2.5	25
148	Phase based venous suppression in resting-state BOLD GE-fMRI. NeuroImage, 2014, 100, 51-59.	4.2	25
149	Diffusion-weighted tractography in the common marmoset monkey at 9.4T. Journal of Neurophysiology, 2017, 118, 1344-1354.	1.8	25
150	Swallowing Preparation and Execution: Insights from a Delayed-Response Functional Magnetic Resonance Imaging (fMRI) Study. Dysphagia, 2017, 32, 526-541.	1.8	25
151	Shape Optimization of an Electric Dipole Array for 7 Tesla Neuroimaging. IEEE Transactions on Medical Imaging, 2019, 38, 2177-2187.	8.9	25
152	Intrinsic functional clustering of anterior cingulate cortex in the common marmoset. NeuroImage, 2019, 186, 301-307.	4.2	25
153	Cortico-Subcortical Functional Connectivity Profiles of Resting-State Networks in Marmosets and Humans. Journal of Neuroscience, 2020, 40, 9236-9249.	3.6	25
154	Reduced brain glutamine in female varsity rugby athletes after concussion and in non oncussed athletes after a season of play. Human Brain Mapping, 2018, 39, 1489-1499.	3.6	24
155	An open access resource for functional brain connectivity from fully awake marmosets. NeuroImage, 2022, 252, 119030.	4.2	23
156	Solvent proton relaxation of aqueous solutions of the serum proteins alpha 2-macroglobulin, fibrinogen, and albumin. Biophysical Journal, 1990, 57, 389-396.	0.5	22
157	Perception of the Mccollough Effect Correlates with Activity in Extrastriate Cortex: A Functional Magnetic Resonance Imaging Study. Psychological Science, 1999, 10, 444-448.	3.3	22
158	Noise properties of a NMR transceiver coil array. Journal of Magnetic Resonance, 2004, 171, 151-156.	2.1	22
159	Neural network of social interaction observation in marmosets. ELife, 2021, 10, .	6.0	22
160	Minimal specifications for non-human primate MRI: Challenges in standardizing and harmonizing data collection. NeuroImage, 2021, 236, 118082.	4.2	22
161	Toward next-generation primate neuroscience: A collaboration-based strategic plan for integrative neuroimaging. Neuron, 2022, 110, 16-20.	8.1	22
162	Comparative study of proton and phosphorus magnetic resonance spectroscopy in schizophrenia at 4 Tesla. Psychiatry Research - Neuroimaging, 2004, 132, 33-39.	1.8	21

#	Article	IF	CITATIONS
163	Hybrid two-dimensional navigator correction: A new technique to suppress respiratory-induced physiological noise in multi-shot echo-planar functional MRI. NeuroImage, 2008, 39, 1142-1150.	4.2	21
164	The Evaluation of Magnesium Chloride within a Polyethylene Glycol Formulation in a Porcine Model of Acute Spinal Cord Injury. Journal of Neurotrauma, 2016, 33, 2202-2216.	3.4	21
165	Morphology-Specific Discrimination between MS White Matter Lesions and Benign White Matter Hyperintensities Using Ultra-High-Field MRI. American Journal of Neuroradiology, 2018, 39, 1473-1479.	2.4	21
166	Direct visualization and characterization of the human zona incerta and surrounding structures. Human Brain Mapping, 2020, 41, 4500-4517.	3.6	21
167	Interaction of Retinal Image and Eye Velocity in Motion Perception. Neuron, 2003, 39, 569-576.	8.1	20
168	Sodium T2*-weighted MR imaging of acute focal cerebral ischemia in rabbits. Magnetic Resonance Imaging, 2004, 22, 983-991.	1.8	20
169	In vivo detection of PARACEST agents with relaxation correction. Magnetic Resonance in Medicine, 2010, 63, 1184-1192.	3.0	20
170	Higher order thalamic nuclei resting network connectivity in early schizophrenia and major depressive disorder. Psychiatry Research - Neuroimaging, 2018, 272, 7-16.	1.8	20
171	Open-source hardware designs for MRI of mice, rats, and marmosets: Integrated animal holders and radiofrequency coils. Journal of Neuroscience Methods, 2019, 312, 65-72.	2.5	20
172	Longitudinal changes of brain microstructure and function in nonconcussed female rugby players. Neurology, 2020, 95, e402-e412.	1.1	20
173	Exogenous Neural Precursor Cell Transplantation Results in Structural and Functional Recovery in a Hypoxic-Ischemic Hemiplegic Mouse Model. ENeuro, 2018, 5, ENEURO.0369-18.2018.	1.9	20
174	Relaxometry model of strong dipolar perturbers for balanced-SSFP: Application to quantification of SPIO loaded cells. Magnetic Resonance in Medicine, 2006, 55, 583-591.	3.0	19
175	Increased deep gray matter iron is present in clinically isolated syndromes. Multiple Sclerosis and Related Disorders, 2014, 3, 194-202.	2.0	19
176	Spontaneous low frequency BOLD signal variations from resting-state fMRI are decreased in Alzheimer disease. PLoS ONE, 2017, 12, e0178529.	2.5	19
177	Linked MRI signatures of the brain's acute and persistent response to concussion in female varsity rugby players. NeuroImage: Clinical, 2019, 21, 101627.	2.7	19
178	Spatial and temporal resolution of functional magnetic resonance imaging. Biochemistry and Cell Biology, 1998, 76, 560-571.	2.0	19
179	Quantitative separation of NMR images of water in wood on the basis of T2. Journal of Magnetic Resonance, 1989, 82, 205-210.	0.5	18
180	Physiological monitoring of small animals during magnetic resonance imaging. Journal of Neuroscience Methods, 2005, 144, 207-213.	2.5	18

#	Article	IF	CITATIONS
181	Progressive membrane phospholipid changes in first episode schizophrenia with high field magnetic resonance spectroscopy. Psychiatry Research - Neuroimaging, 2012, 201, 25-33.	1.8	18
182	Reliable RF B/E-Field Probes for Time-Domain Monitoring of EM Exposure During Medical Device Testing. IEEE Transactions on Antennas and Propagation, 2017, 65, 4815-4823.	5.1	18
183	Radiofrequency coil for routine ultraâ€highâ€field imaging with an unobstructed visual field. NMR in Biomedicine, 2021, 34, e4457.	2.8	18
184	NMR Simulation Analysis of Statistical Effects on Quantifying Cerebrovascular Parameters. Biophysical Journal, 2007, 92, 1014-1021.	0.5	17
185	Longitudinal 4.0ÂTesla 31P magnetic resonance spectroscopy changes in the anterior cingulate and left thalamus in first episode schizophrenia. Psychiatry Research - Neuroimaging, 2009, 173, 155-157.	1.8	17
186	Effects of MP2RAGE B1+ sensitivity on inter-site T1 reproducibility and hippocampal morphometry at 7T. NeuroImage, 2021, 224, 117373.	4.2	17
187	Effects of phase regression on high-resolution functional MRI of the primary visual cortex. NeuroImage, 2021, 227, 117631.	4.2	15
188	Simultaneous functional MRI of two awake marmosets. Nature Communications, 2021, 12, 6608.	12.8	15
189	High-temporal-resolution studies of the human primary visual cortex at 4 T: Teasing out the oxygenation contribution in FMRI. International Journal of Imaging Systems and Technology, 1995, 6, 209-215.	4.1	14
190	Transceive surface coil array for MRI of the human prostate at 4T. Magnetic Resonance in Medicine, 2007, 57, 455-458.	3.0	14
191	A geometrically adjustable receive array for imaging marmoset cohorts. NeuroImage, 2017, 156, 78-86.	4.2	14
192	Functional reorganization during the recovery of contralesional target selection deficits after prefrontal cortex lesions in macaque monkeys. NeuroImage, 2020, 207, 116339.	4.2	14
193	Muting, not fragmentation, of functional brain networks under general anesthesia. NeuroImage, 2021, 231, 117830.	4.2	14
194	Automatic determination of the regularization weighting for waveletâ€based compressed sensing MRI reconstructions. Magnetic Resonance in Medicine, 2021, 86, 1403-1419.	3.0	14
195	Mesoscale hierarchical organization of primary somatosensory cortex captured by resting-state-fMRI in humans. NeuroImage, 2021, 235, 118031.	4.2	14
196	Venocentric Lesions: An MRI Marker of MS?. Frontiers in Neurology, 2013, 4, 98.	2.4	13
197	Initial Investigation into Microbleeds and White Matter Signal Changes following Radiotherapy for Low-Grade and Benign Brain Tumors Using Ultra-High-Field MRI Techniques. American Journal of Neuroradiology, 2017, 38, 2251-2256.	2.4	13
198	Implementation issues of multivoxel STEAM-localized1H spectroscopy. Magnetic Resonance in Medicine, 2005, 53, 713-718.	3.0	12

#	Article	IF	CITATIONS
199	Robust prescan calibration for multiple spin-echo sequences: application to FSE and b-SSFP. Magnetic Resonance Imaging, 2006, 24, 857-867.	1.8	12
200	Mental chronometry. NeuroImage, 2012, 62, 1068-1071.	4.2	12
201	Magnetic field probes for timeâ€domain monitoring of RF exposure within tissueâ€mimicking materials for MRIâ€compatible medical device testing. Electronics Letters, 2018, 54, 16-18.	1.0	12
202	In vivo manganese tract tracing of frontal eye fields in rhesus macaques with ultra-high field MRI: Comparison with DWI tractography. NeuroImage, 2018, 181, 211-218.	4.2	12
203	Dynamic Reconfiguration, Fragmentation, and Integration of Whole-Brain Modular Structure across Depths of Unconsciousness. Cerebral Cortex, 2020, 30, 5229-5241.	2.9	12
204	Normative Analysis of Individual Brain Differences Based on a Population MRI-Based Atlas of Cynomolgus Macaques. Cerebral Cortex, 2021, 31, 341-355.	2.9	12
205	Highcor: A novel data-driven regressor identification method for BOLD fMRI. NeuroImage, 2014, 98, 184-194.	4.2	11
206	Comparison of Multiecho Postprocessing Schemes for SWI with Use of Linear and Nonlinear Mask Functions. American Journal of Neuroradiology, 2014, 35, 38-44.	2.4	11
207	The functional scout image: Immediate mapping of cortical function at 4 tesla using receiver phase cycling. Magnetic Resonance in Medicine, 1997, 38, 183-186.	3.0	10
208	Influence of hypoxia on wavelength dependence of differential pathlength and near-infrared quantification. Physics in Medicine and Biology, 2002, 47, 1573-1589.	3.0	10
209	SENSE optimization of a transceive surface coil array for MRI at 4 T. Magnetic Resonance in Medicine, 2006, 56, 630-636.	3.0	10
210	Spared somatomotor and cognitive functions in a patient with a large porencephalic cyst revealed by fMRI. Neuropsychologia, 2004, 42, 405-418.	1.6	9
211	Concentric radiofrequency arrays to increase the statistical power of resting-state maps in monkeys. NeuroImage, 2018, 178, 287-294.	4.2	9
212	Concussion Acutely Decreases Plasma Glycerophospholipids in Adolescent Male Athletes. Journal of Neurotrauma, 2021, 38, 1608-1614.	3.4	9
213	SchrĶdinger filtering: a precise EEG despiking technique for EEG-fMRI gradient artifact. NeuroImage, 2021, 226, 117525.	4.2	8
214	Optimized MRI contrast for onâ€resonance proton exchange processes of PARACEST agents in biological systems. Magnetic Resonance in Medicine, 2009, 62, 1282-1291.	3.0	7
215	High Rate of Microbleed Formation following Primary Intracerebral Hemorrhage. International Journal of Stroke, 2015, 10, 1187-1191.	5.9	7
216	General Coupling Matrix Synthesis Pub _newline ? for Decoupling MRI RF Arrays. IEEE Transactions on Medical Imaging, 2016, 35, 2229-2242.	8.9	7

#	Article	IF	CITATIONS
217	Interâ€echo variance as a weighting factor for multiâ€channel combination in multiâ€echo acquisition for local frequency shift mapping. Magnetic Resonance in Medicine, 2015, 73, 1654-1661.	3.0	6
218	Prediction of radiation necrosis in a rodent model using magnetic resonance imaging apparent transverse relaxation (\$R_{2}^{*}\$). Physics in Medicine and Biology, 2018, 63, 035010.	3.0	6
219	Protocol-dependence of middle cerebral artery dilation to modest hypercapnia. Applied Physiology, Nutrition and Metabolism, 2021, 46, 1038-1046.	1.9	6
220	Functional Imaging of the Brain by Nuclear Magnetic Resonance. , 1994, , 137-150.		6
221	A Canadian Perspective on Ethics Review and Neuroimaging: Tensions and Solutions. Canadian Journal of Neurological Sciences, 2011, 38, 572-579.	0.5	5
222	Analysis of circumferential shielding as a methodto decouple radiofrequency coils for highâ€field MRI. Concepts in Magnetic Resonance Part B, 2013, 43B, 11-21.	0.7	5
223	Apparent transverse relaxation () on <scp>MRI</scp> as a method to differentiate treatment effect (pseudoprogression) versus progressive disease in chemoradiation for malignant glioma. Journal of Medical Imaging and Radiation Oncology, 2018, 62, 224-231.	1.8	5
224	Using variableâ€rate selective excitation (VERSE) radiofrequency pulses to reduce power deposition in pulsed arterial spin labeling sequence at 7 Tesla. Magnetic Resonance in Medicine, 2020, 83, 645-652.	3.0	5
225	Brain Metabolite Levels in Sedentary Women and Non-contact Athletes Differ From Contact Athletes. Frontiers in Human Neuroscience, 2020, 14, 593498.	2.0	5
226	Spatial and temporal resolution in fMRI. , 2001, , 146-158.		5
227	Reduced visual evoked responses in multiple sclerosis patients with optic neuritis: Comparison of functional magnetic resonance imaging and visual evoked potentials. Multiple Sclerosis Journal, 1999, 5, 161-164.	3.0	5
228	Integration of an RF coil and commercial field camera for ultrahighâ€field MRI. Magnetic Resonance in Medicine, 2022, 87, 2551-2565.	3.0	5
229	A cradle-shaped gradient coil to expand the clear-bore width of an animal MRI scanner. Physics in Medicine and Biology, 2010, 55, 497-514.	3.0	4
230	Susceptibilityâ€weighted imaging using interâ€echoâ€variance channel combination for improved contrast at 7 tesla. Journal of Magnetic Resonance Imaging, 2017, 45, 1113-1124.	3.4	4
231	Scene classification and parahippocampal place area activation in an individual with visual form agnosia. Journal of Vision, 2010, 2, 495-495.	0.3	3
232	Putative Concussion Biomarkers Identified in Adolescent Male Athletes Using Targeted Plasma Proteomics. Frontiers in Neurology, 2021, 12, 787480.	2.4	3
233	A lowâ€cost, mechanically simple apparatus for measuring eddy currentâ€induced magnetic fields in MRI. NMR in Biomedicine, 2013, 26, 1285-1290.	2.8	2
234	Functional Imaging of Auditory Cortex in Adult Cats using High-field fMRI. Journal of Visualized Experiments, 2014, , e50872.	0.3	2

#	Article	IF	CITATIONS
235	Structural alterations in cortical and thalamocortical white matter tracts after recovery from prefrontal cortex lesions in macaques. NeuroImage, 2021, 232, 117919.	4.2	2
236	Human forebrain activation by visceral stimuli. Journal of Comparative Neurology, 1999, 413, 572-582.	1.6	2
237	Visually-guided grasping produces fMRI activation in dorsal but not ventral stream brain areas. Journal of Vision, 2010, 1, 194-194.	0.3	2
238	Resonate: Reflections and recommendations on implicit biases within the ISMRM. Journal of Magnetic Resonance Imaging, 2019, 49, 1509-1511.	3.4	1
239	Elimination of lowâ€inversionâ€efficiency induced artifacts in wholeâ€brain MP2RAGE using multiple RFâ€shim configurations at 7 T. NMR in Biomedicine, 2020, 33, e4387.	2.8	1
240	Demonstration and suppression of respirationâ€related artifacts in Bloch–Siegert shiftâ€based B 1 + maps of the human brain. NMR in Biomedicine, 2020, 33, e4299.	2.8	1
241	Functional Organization of Frontoparietal Cortex in the Marmoset Investigated with Awake Resting-State fMRI. Cerebral Cortex, 2022, 32, 1965-1977.	2.9	1
242	Comparison of T2*-weighted sequences for functional MRI. International Journal of Imaging Systems and Technology, 1995, 6, 184-190.	4.1	0
243	The employment of the insane. British Journal of Psychiatry, 2000, 176, 401-401.	2.8	0
244	Reply. Annals of Neurology, 2013, 73, 797-797.	5.3	0
245	Editorial Focus on "Invariant and heritable local cortical organization as revealed by fMRI― Journal of Neurophysiology, 2018, 120, 758-759.	1.8	0
246	Author Response: Longitudinal Changes of Brain Microstructure and Function in Nonconcussed Female Rugby Players. Neurology, 2021, 96, 968.2-969.	1.1	0
247	Receiver phase alignment using fitted SVD derived sensitivities from routine prescans. PLoS ONE, 2021, 16, e0256700.	2.5	0
248	Areas active during a pointing but not a saccade delay are medial to saccade-and-pointing network. Journal of Vision, 2010, 1, 265-265.	0.3	0
249	Differing viewpoint effects in the ventral and dorsal visual streams revealed using fMRI. Journal of Vision, 2010, 2, 45-45.	0.3	0
250	Visual and haptic object priming have a similar effect on fMRI activation in extra-striate cortex james@cerco.ups-tlse.fr. Journal of Vision, 2010, 1, 483-483.	0.3	0
251	Afterimages and pursuit: refining Helmholtz's theory of visual motion perception. Journal of Vision, 2010, 3, 602-602.	0.3	0